Journal of Nuclear Materials 406 (2010) 351–355

Contents lists available at ScienceDirect

Journal of Nuclear Materials

journal homepage: www.elsevier.com/locate/jnucmat

Vacancy formation and solid solubility in the U–Zr–N system

Merja Pukari *, Odd Runevall, Nils Sandberg, Jan Wallenius

Reactor Physics, Royal Institute of Technology, Albanova University Center, S-106 91 Stockholm, Sweden

ARTICLE INFO

Article history:
Received 29 March 2010
Accepted 8 September 2010

ABSTRACT

For the purpose of developing a nuclear fuel with enhanced thermophysical properties and better irradiation performance density functional theory calculations are used to explore UN, ZrN and (U,Zr)N. Negative deviation of ground state energy from the ideal solution model as well as energetically favourable maximal distance between substitutional metal atoms in respective nitrides indicate mutual solubility of UN and ZrN at all temperatures. Nitrogen vacancy formation energies in UN (1.81 eV) and ZrN (1.40 eV) are considerably lower than metal vacancy formation energies. A substitutional Zr atom in UN has little effect on nitrogen vacancy formation energies (~1.79 eV), while U in ZrN decreases the value by ~0.1 eV (~1.30 eV) due to elastic stress and charge density redistribution in the material. The relative distance between a substitutional metal atom and a vacancy in UN has little influence over the radially declining displacement pattern induced by the substitutional atom, while in ZrN the relaxation of atoms is governed by the position of the vacancy. The calculated vacancy formation energies indicate a lower surface energy of ZrN in comparison with UN.

1. Introduction

Generation-IV reactors could utilise nuclear fuels which exhibit numerous better attributes than the currently predominant oxide fuels. Uranium nitride, for instance, has high thermal conductivity [1–3] and melting temperature [4], good liquid metal compatibility [5] and breeding performance [5,6]; but has often been discarded due to its incompatibility with water [4,7] and relatively low dissociation temperature [8–10]. The cost of ^{15}N enrichment, necessary to avoid production of ^{14}C, is a further drawback [11]. However, in solution with ZrN actinide nitrides have shown relatively good swelling behaviour and extremely low fission gas release [10]. The addition of ZrN to UN also increases the dissociation temperature sufficiently to exclude it as a threat to safe reactor performance [12,13].

Other authors have employed density functional theory (DFT) calculations [14] to analyse defect formation in UN [15–18] and the behaviour of ZrN lattice under nitrogen deficiency [19]. The latter has shown to have little influence over lattice parameters in both nitrides [15,20].

On the other hand, vacancy formation studies have not been reported in neither ZrN nor (U,Zr)N. Moreover, earlier experimental work, where the influence of C and O impurities is difficult to determine, has resulted in a discrepancy on whether UN and ZrN are mutually soluble [21,22]. Both questions need to be answered to be able to interpret diffusion experiments in these materials, simulate fuel performance and tailor production processes.

The current study aims to clarify trends for nitrogen vacancy formation in UN, ZrN and (U,Zr)N of either U or Zr majority. In addition, the paper employs DFT-calculations for the purpose of analysing mutual solubility of UN and ZrN since a theoretical approach permits one to exclude the impact of C and O impurities.

2. Methods

Both UN and ZrN have the rock-salt crystal structure, with the respective lattice constants $a_{0,UN} = 4.88$ Å [9] and $a_{0,ZrN} = 4.58$ Å [20] at room temperature. According to the the assumption made by Benedict [23], these materials are expected to be fully soluble, since $a_{0,UN}$ exceeds $a_{0,ZrN}$ of the same crystal structure by less than 8.5%.

The rock-salt crystal structure in our DFT-calculations is described by a supercell of either 64 or 128 metal (M) and nitrogen (N) atoms. The former is constructed from $2 \times 2 \times 2$ unit cells and is used due to the benefit of being easily visualised while offering a suitable supercell size. The 128-atom supercell, selectively used in calculations, is derived from a primitive face-centered cubic cell and expanded with translation vectors $(4 \times 4 \times 4)$.

A system representing solid solution between UN and ZrN with either U or Zr majority has been constructed by substituting one or two atoms of the dominant metal species with atoms of the other metal species. Thus, the notations used are $U_{31}Zr_1N_{32}$ for a mixed nitride of 96.87% U majority and $U_1Zr_{31}N_{32}$ for an equivalent Zr

* Corresponding author.
E-mail address: pukari@kth.se (M. Pukari).

0022-3115/$ - see front matter © 2010 Elsevier B.V. All rights reserved.
doi:10.1016/j.jnucmat.2010.09.006

majority in the case of a 64-atom system. Single atom substitution in a 128-atom system corresponds to 98.44% majority, indicated with $U_{63}Zr_1N_{64}$ and $U_1Zr_{63}N_{63}$. Likewise, a system with the majority of 93.75% of either metal species is constructed by substituting two corresponding metal atoms in a 64-atom system, in which case notations $U_{30}Zr_2N_{32}$ and $U_2Zr_{30}N_{32}$ are used. Resulting configurations that arise from introducing more than one defect are described below.

Vacancies are created by removing any one M or N atom from UN and ZrN. In the case of $U_{31}Zr_1N_{31}$ and $U_1Zr_{31}N_{31}$, N vacancies can be created at 4 unique distances in relation to the position of the substitutional M atom in a 64-atom system. These distances correspond to $0.5a_0$ (I), $0.86a_0$ (II), $1.12a_0$ (III) and $1.5a_0$ (IV) in a cubic supercell of $2a_0$ side length and are indicated with corresponding roman numerals.

Similarly, the two substitutional metal atoms in $U_{30}Zr_2N_{32}$ and $U_2Zr_{30}N_{32}$ in a 64-atom system can be organized in 5 unique configurations, regarding their distance to each other. These configurations are represented with letters (a)–(e) in this paper, corresponding to the distances of $0.70a_0$(a), $1.00a_0$ (b), $1.22a_0$(c), $1.42a_0$(d) and $1.75a_0$(e) in the aforementioned system.

The 64-atom system has further been used to investigate the validity of Vegard's law in $U_{1-x}Zr_xN$ by performing volume relaxation calculations on intermediate compositions where the distance between substitutional atoms has been kept maximal. The approach was chosen due to calculations indicating preferential maximal distance between U atoms in a mixed nitride (Section 3.1), which does not necessarily represent the ground states but serves as an approximation.

Vacancy formation energies $E_{f,va}$ are calculated according to [24]:

$$E_{f,va} = E_v - E_b + \sum_{i=1} n_i \mu_i \quad (1)$$

where E_v is the energy of a supercell containing a vacancy, E_b the energy of a bulk supercell, n_i the number of atoms of a particular element removed, μ_i represents the chemical potential of a particular element and has been defined in two ways. (i) The chemical potentials of U, Zr and N in the given calculations are assumed to be equal to $E_b \cdot n^{-1}$. The named approach can be shown to provide a value for the chemical potential which is within physically sound limits [25], but is not entirely comparable with the work of other authors [15–18]. For the reason of comparison, (ii) the chemical potential of an element is also defined as being equal to the energy of a single isolated atom.

The matter of solubility of UN and ZrN is addressed by studying the mixing energy ΔE_{mix} of UN and ZrN per formula unit (FU), which is defined as the deviation between the ground state energy of a particular composition and the presumable ground state energy derived from the ideal solution model Eq. (2). The latter assumes a linear relationship between the ground state energies of UN and ZrN at 0 K [26] as shown below:

$$\Delta E_{mix} = \frac{E_{U_{1-x}Zr_x} - (1-x)\cdot E_{UN} + x \cdot E_{ZrN}}{n_{FU}} \quad (2)$$

Here $E_{U_{1-x}Zr_x}$ represents the total energy for a particular mixed nitride composition obtained from the DFT-calculations, E_{UN} and E_{ZrN} the energy for pure UN and ZrN, respectively, and n_{FU} the number of nitride formula units.

The presented first-principles calculations have been conducted with the DFT plane-wave basis set computer code VASP 4.6 [27,28]. All calculations employ the scalar relativistic projector augmented wave (PAW) pseudopotentials [29] to describe the core electrons. Both generalised gradient approximation (GGA) [30] and local density approximation (LDA) [31] pseudopotentials are used in calculations, where the number of valence electrons for U, Zr and N is 14, 4 and 5 in the case of GGA; and 14, 12 and 5 in the case of LDA, respectively. The plane wave cut-off energy is set to 500 eV in all calculations. A Monkhorst–Pack integration [32] set-up with a $3 \times 3 \times 3$ k-point mesh in the Brillouin zone showed sufficient convergence in supercell calculations. For determining the total energy of systems, the convergence criterion is set so that the energy difference between two consecutive steps is less than 10^{-5} eV for electronic relaxations and less than 10^{-4} eV for ionic relaxations.

In general, volume relaxation is excluded from the current calculations, since previous work has shown even high vacancy concentration to have a negligible influence on lattice parameters [15,19,20,22]. Volume relaxation has been allowed only in specific cases in order to control the validity of the results and is in this case clearly stated.

To a large extent spin-polarisation is omitted in the current study since ZrN is a non-magnetic material and the ground state of UN is non-magnetic at any temperature relevant for fuel applications [33]. Therefore results from an anti-ferromagnetic set-up are seen to be of little practical value in nuclear fuel development. Magnetic calculations are performed to check the reliability of the set-up against earlier work and to investigate the magnetic set-up of mixed nitrides at 0 K.

3. Results

The lattice parameters of both stoichiometric nitrides obtained from DFT calculations with GGA pseudopotentials ($a_{0,UN}$ = 4.86 Å and $a_{0,ZrN}$ = 4.61 Å) are in good agreement with experimental values and with previously reported results from DFT calculations [15,19]. This applies only partially for calculations with LDA pseudopotentials, since the theoretical $a_{0,UN}$ deviates by 2.5% from experimental values ($a_{0,UN}$ = 4.77 Å and $a_{0,ZrN}$ = 4.55 Å). It has been previously shown that LDA pseudopotentials underestimate lattice parameters and overestimate bulk moduli [34]. The bulk moduli of UN (K_{UN} = 209 GPa) and ZrN (K_{ZrN} = 262 GPa) are overestimated by 17% [35] and 8% [36] with GGA pseudopotentials.

Lattice parameters for all mixed nitrides are initially determined from Vegard's law [37], the validity of which for these materials is subsequently verified by allowing the volumes to relax. Deviation between the assumed lattice parameter and that obtained from full volume relaxation is in the order of 0.1% for systems focused on in this study. The maximal deviation of 0.23% between lattice parameters occurs at $U_{0.5}Zr_{0.5}N$ (see Fig. 1). The results are well in line with experimental observations of (U,Zr)N closely following Vegard's law [22]. A single Zr substitution introduces a defect volume $\Delta V = -0.66$ Å^3 in UN, and a single U substitution in ZrN a defect volume $\Delta V = 0.40$ Å^3. The preliminary calculations have shown that the ground states of UN and ZrN are metallic, since the density of states at the Fermi surface is non-zero for both nitrides.

3.1. Solubility of UN and ZrN

The matter of full solubility between UN and ZrN is addressed with Fig. 2. The three different concentrations in Fig. 2 are modelled as described in Section 2 and indicate full solubility as the DFT-obtained total energy of a mixed nitride of a particular composition is lower than the energy of the same composition from the ideal solution model. Furthermore, mixing energies for $U_2Zr_{30}N_{32}$ (at $x = 0.063$) decrease with increasing distance between the substitutional U atoms, which is consistent with long range order and hence invalidates the assumption of a miscibility gap. Additionally highly ordered systems representing intermediate compositions were investigated, all resulting in a negative mixing energy.

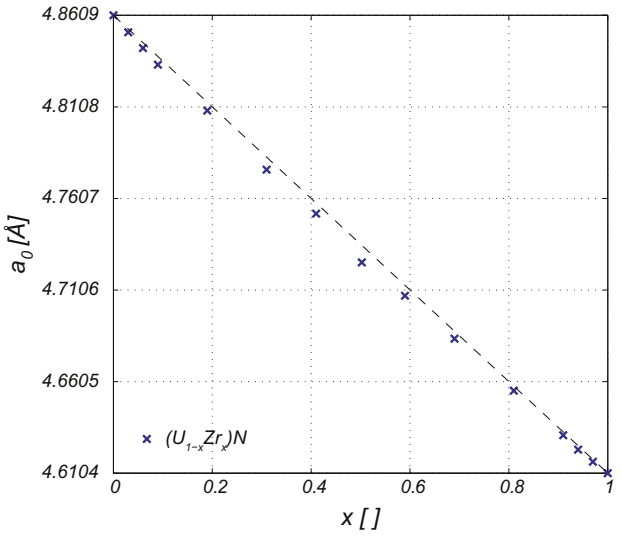

Fig. 1. The validity of Vegard's law in $U_{1-x}Zr_xN$, where the dashed line represents a linear relationship between $a_{0,UN}$ and $a_{0,ZrN}$.

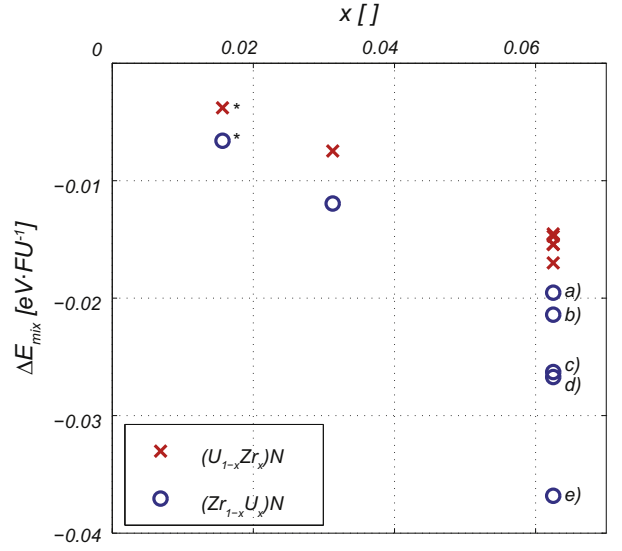

Fig. 2. Mixing energy of UN and ZrN in relation to the ideally linear correlation between them, ΔE_{mix}(eV FU^{-1}). Values marked with (*) indicate results from 128-atom systems. Values marked with letters a–e represent five unique distances between two substitutional metal atoms in a mixed nitride and are sorted by increasing distance.

The results from given configurations suggest the existence of one or several ordered intermetallic structures. The calculations illustrate solubility at 0 K, yet the mixing ought to be even more pronounced at higher temperatures due to the entropy contribution. Interdistance between substitutional metal atoms in $U_{30}Zr_2N_{32}$ (at $x = 0.063$) has no measurable effect on the energies. The previous statements also bear a significance if one were to perform alternative calculations on (U,Zr)N, e.g. employ larger super-cells or include a higher amount of substitutional metal atoms.

3.2. Vacancy formation energies

Table 1 summarises formation energies $E_{f,va}$ for M and N vacancies in pure UN and ZrN, using GGA and LDA pseudopotentials. It is evident that nitrogen deficiency is more favourable than that of a metal, regardless of the potentials used. The same trend has been noted by other authors [15–18] when calculating $E_{f,va}$ according to the (ii) definition of the chemical potentials. The phenomenon is in good agreement with experimental results, which claim that mononitrides of U and Zr have rather deficiency than excess of nitrogen [20,38,39]. Consequently, the metallic vacancy formation is not studied in mixed nitrides. Table 1 also presents values for spin-polarised calculations, which are a more appropriate estimation at 0 K. The values are in line with the non-magnetic calculations, although with a slightly more pronounced range between the formation energies of M and N vacancies.

Table 1
Vacancy formation energies $E_{f,va}$ (eV) for nitrogen (N) and metal (M) atoms in UN and ZrN for a 64-atom supercell, according to Eq. (1). Values in brackets given for a 128-atom supercell. (i) $\mu_i = E_b \cdot n^{-1}$ (ii) μ_i is equal to the energy of an isolated atom.

		GGA non-magnetic		Magnetic	LDA non-magnetic	
		UN	ZrN	UN	UN	ZrN
(i)	N	1.87 (1.81)	1.31 (1.40)	1.74	1.61	1.43
	M	3.24	1.59	3.29	3.87	2.17
(ii)	N	9.77 (9.71)	8.33 (8.42)	9.65	10.76	9.50
	M	10.05	9.75	10.10	11.84	11.48

The values in Table 1 suggest that a nitrogen vacancy is energetically more favourable in ZrN than in UN. Tight binding bond-breaking models for vacancy and surface formation energies in metals and metal carbides result in the following relations [40,41]

$$E_{va} \simeq C_B \frac{\sqrt{C_B} - \sqrt{C_B - 1}}{\sqrt{C_B}} E_{coh} \quad (3)$$

$$E_{surf} \simeq \frac{\sqrt{C_B} - \sqrt{C_S}}{\sqrt{C_B}} E_{coh} \quad (4)$$

where C_B and C_S are the coordination numbers in the bulk and at the surface, respectively.

Hence, in materials where tight binding models are applicable, surface energies tend to be proportional to vacancy formation energies. Considering the metallic character of the here considered nitride compounds, one may speculate that the surface energy of ZrN should be lower that than of UN, having important implications for the composition of surfaces in (U,Zr)N. The latter is relevant in the present context since the stabilising and protective properties of ZrN may act more efficiently if surfaces of (U,Zr)N grains and fuel pellets were enriched in ZrN, as compared to the bulk composition. This conjecture is strengthened by the calculated di-vacancy (M + N) energy of 2.65 eV in ZrN, being considerably lower than that of UN (4.33 eV). This further poses a question of how the vacancy formation mechanism in UN and ZrN is altered if substitutional Zr and U atoms are introduced to the materials.

Thus, Table 2 summarises N vacancy formation energies in $U_{31}Zr_1N_{32}$ and $U_{63}Zr_1N_{64}$; as well as in $U_1Zr_{31}N_{32}$ and $U_1Zr_{63}N_{64}$, calculated with GGA and LDA pseudopotentials for magnetic and non-magnetic set-ups. Here the magnetic calculations for $U_1Zr_{31}N_{32}$ appear to be indistinguishable from the non-magnetic calculations of the same composition, whereas the magnetic calculations in $U_{31}Zr_1N_{32}$ are rather akin to the magnetic pure UN.

In the case of $U_{31}Zr_1N_{32}$, increasing distance between the substitutional metal atom and a vacancy has no measurable effect. As expected, the vacancy formation energies are comparable with a pure UN. The variation in results cannot be claimed to be introduced due to the substitutional Zr atom, although a decrease in vacancy formation energies due to it was initially expected by the authors. Calculations with a 128-atom system confirm these results. On the other hand, vacancy formation energies in $U_1Zr_{31}N_{32}$ bring up two unanticipated effects.

Table 2
Vacancy formation energies $E_{f,va}$ (eV) for nitrogen (N) in mixed nitrides, according to Eq. (1). Roman numerals indicate 4 unique configurations in a 64-atom supercell. (*) numerical artifact, (**) decrease of ca 0.1 eV compared to pure ZrN due to a substitutional U atom. (i) $\mu_i = E_b \cdot n^{-1}$ (ii) μ_i is equal to the energy of an isolated atom.

		GGA						LDA	
		Non-magnetic				Magnetic		Non-magnetic	
		$U_{31}Zr_1N_{32}$	$U_{63}Zr_1N_{64}$	$U_1Zr_{31}N_{32}$	$U_1Zr_{63}N_{64}$	$U_{31}Zr_1N_{32}$	$U_1Zr_{31}N_{32}$	$U_{31}Zr_1N_{32}$	$U_1Zr_{31}N_{32}$
(i)	I	1.78	1.77	1.73*	1.30**	1.71	1.73	1.63	1.92
	II	1.84	1.80	1.20**	1.30**	1.74	1.20	1.57	1.32
	III	1.88	1.80	1.23**	1.32**	1.78	1.23	1.64	1.37
	IV	1.86	1.78	1.20**	1.29**	1.77	1.20	1.59	1.32
(ii)	I	9.66	9.66	8.78*	8.34**	9.60	8.78	10.62	9.90
	II	9.73	9.70	8.25**	8.34**	9.63	8.25	10.56	9.29
	III	9.76	9.70	8.28**	8.37**	9.67	8.28	10.63	9.34
	IV	9.75	9.67	8.26**	8.33**	9.66	8.26	10.58	9.30

The value of $E_{f,va}$ is significantly higher in configuration I (*), compared to the other set-ups, and furthermore exceeds that of a pure ZrN. This suggests that N atoms closest to the substitutional U behave as in UN, presumably due to a stronger binding between U and N than Zr and N. This particular calculation was repeated with volume relaxation, in order to detect a potentially incorrect set-up, but resulted in an equal outcome. As can be seen in Table 2, calculations with a 128-atom supercell with an equivalent configuration of $U_1Zr_{63}N_{64}$ do not confirm this result. It is likely that a lattice-setup with three species and a nitrogen vacancy in the $2 \times 2 \times 2$ cubic supercell leads to a numerical artifact in configuration I, due to periodic boundary conditions, i.e. interaction between mirror images of the defect.

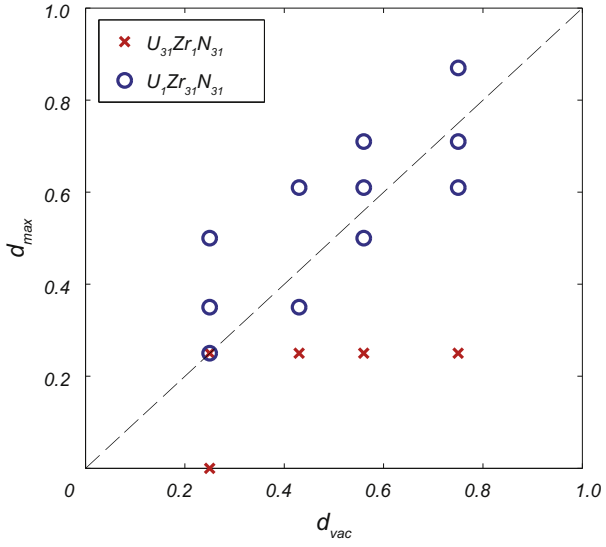

Fig. 3. Substitutional atom induced atomic displacement patterns in UN and ZrN. [0,0] marks the position of the substitutional metal atom; d_{max} – the distance of an atom with the maximal displacement magnitude from the substitutional metal atom; d_{va} – the distance of a N vacant site from the substitutional metal atom. On both axis, $2 \cdot a_0 = 1$ of the particular material.

3.3. Atomic displacements

Comparison of N vacancy formation energies in Tables 1 and 2 shows that a single U substitution in ZrN decreases these energies by on average 0.1 eV, while a Zr substitution in UN has no such effect. This is further investigated by examining the atomic displacements in the two systems, obtained by relaxing the cells. Thus, the distance of the atom with the largest displacement (d_{max}) is plotted as a function of the distance of the N vacancy from the substitutional atom (d_{va}) in Fig. 3. The two emerging patterns show that (a) in $U_{31}Zr_1N_{31}$, nearest neighbours to the Zr substitutional atom undergo maximal displacement, but that (b) in $U_1Zr_{31}N_{31}$, nearest neighbours to the N vacancy undergo maximal displacement. It is presumably the considerably larger U atom in $U_1Zr_{31}N_{31}$ that introduces stress to the system, alternates the manner for the cell to relax and hence reduces the vacancy formation energies.

The difference between $U_{31}Zr_1N_{32}$ and $U_1Zr_{31}N_{32}$ can further be understood from the charge densities of the two systems. In Fig. 4 the deviation in charge density between the ground state of $U_1Zr_{31}N_{32}$ and the superposition of atomic orbitals is depicted for two (001) planes in the crystal. The U substitution evidently dis-

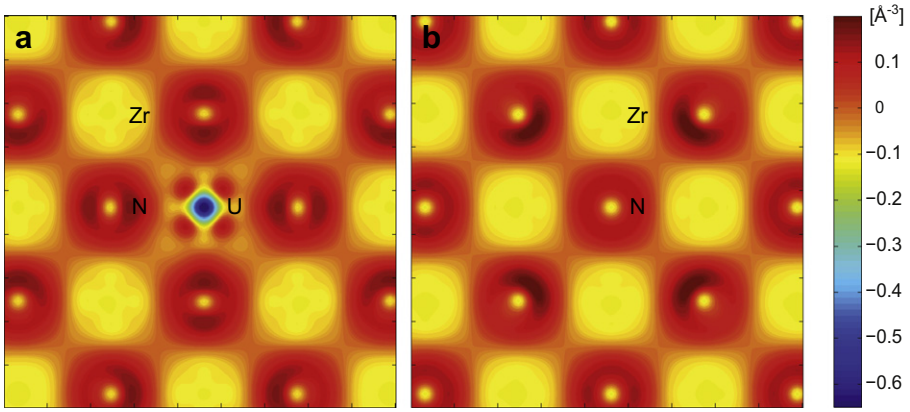

Fig. 4. Difference of electronic charge density in $U_1Zr_{31}N_{32}$ between a fully relaxed system and a superposition of the charge, given on a (001) plane with (a) the U substitution on the same plane and (b) at a $0.5a_0$ distance from the U atom.

torts the charge density distribution by donating electrons to neighbouring N atoms, having such an influence on N atoms throughout the supercell. It is then noteworthy that the charge densities of $U_{31}Zr_1N_{32}$ showed no asymmetrical deviations.

4. Conclusion

The current study has employed DFT computational methods in order to illustrate mutual solubility of UN and ZrN at 0 K and finite temperatures. The trends in calculated vacancy formation energies are in line with experiments, which suggest that it is more likely to produce UN and ZrN with nitrogen than metal deficiency and that ZrN is significantly more hypostoichiometric than UN. The inclusion of U in ZrN is likely to ease the production of hypostoichiometric materials, as it decreases the vacancy formation energies. The paper shows that in a complex set-up of defects in compounds too small of cell sizes (64 atoms in this case) may introduce numerical artifacts. The spin-polarized and non-spin polarized results in this paper do not differ significantly.

Acknowledgements

Financial support from Vetenskapsrådet (Contract No. 90399101, GENIUS) is acknowledged. The authors would like to thank Swedish National Infrastructure for Computing (SNIC) for allocation of computing resources and Pavel Korzhavyi for insights into the art of DFT-calculations.

References

[1] S. Hayes, J. Thomas, K. Peddicord, J. Nucl. Mater. 171 (1990) 289–299.
[2] T. Kikuchi, T. Takahashi, S. Nasu, J. Nucl. Mater. 45 (1973) 284–292.
[3] Y. Suzuki, Y. Arai, J. Alloys Compd. 271–273 (1998) 577–582.
[4] S. Sunder, N.H. Miller, J. Alloys Compd. 271–273 (1998) 568–572.
[5] H. Bailly, D. Menessier, C. Prunier, The Nuclear Fuel of Pressurized Water Reactors and Fast Reactors: Design and Behaviour, Intercept Ltd., 1999.
[6] B.D. Rogozkin, N.M. Stepennova, A.A. Proshkin, Atom. Energy 95 (2003) 624–636.
[7] G. Rao, S. Mukerjee, V. Vaidya, V. Venugopal, D. Sood, J. Nucl. Mater. 185 (1991) 231–241.
[8] T. Ogawa, F. Kobayashi, T. Sato, R.G. Haire, J. Alloys Compd. 271–273 (1998) 347–354.
[9] H. Tagawa, J. Nucl. Mater. 51 (1974) 78–89.
[10] J. Wallenius, CONFIRM: final technical report: collaboration on nitride fuel irradiation and modelling, Technical Report, Kungliga Tekniska Högskolan, 2009.
[11] CEA, Carbon 14 production and Nitrogen 15 enrichment of nitride fuels, Technical Report, Laboratoire des irradiations, 2001.
[12] R. Thetford, M. Mignanelli, J. Nucl. Mater. 320 (2003) 44–53.
[13] T. Ogawa, M. Akabori, J. Alloys Compd. 213–214 (1994) 173–177.
[14] W. Kohn, L.J. Sham, Phys. Rev. 140 (1965) A1133–A1138.
[15] E.A. Kotomin, R.W. Grimes, Y. Mastrikov, N.J. Ashley, J. Phys. Condens. Matter 19 (2007) 106208.
[16] E.A. Kotomin, Y.A. Mastrikov, Y.F. Zhukovskii, P.V. Uffelen, V.V. Rondinella, Phys. Status Solidi C 4 (2007) 1193–1196.
[17] E. Kotomin, Y. Mastrikov, J. Nucl. Mater. 377 (2008) 492–495.
[18] E. Kotomin, D. Gryaznov, R. Grimes, D. Parfitt, Y. Zhukovskii, Y. Mastrikov, P.V. Uffelen, V. Rondinella, R. Konings, Nucl. Instrum. Methods Phys. Res., Sect. B 266 (2008) 2671–2675.
[19] N.J. Ashley, R.W. Grimes, K.J. McClellan, J, Mater. Sci. 42 (2007) 1884–1889.
[20] A.N. Christensen, S. Fregerslev, Acta Chem. Scand. Ser. A 31 (1977) 861–868.
[21] H. Holleck, in: Conference: Symposium on Thermodynamics of Nuclear Materials, Vienna, Austria, 21 October 1974, CONF-741030–P2, Kernforschungszentrum, Karlsruhe, Germany, International Atomic Energy Agency, Vienna, 1975, pp. 213–264.
[22] M. Walter, J. Somers, A. Fernndez-Carretero, J. Rothe, J. Nucl. Mater. 373 (2008) 90–93.
[23] U. Benedict, The solubility of solid fission products in carbides and nitrides of uranium and plutonium, part ii: solubility rules based on lattice parameter differences, Technical Report EUR 5766EN, IAEA, 1977.
[24] P. Nerikar, T. Watanabe, J.S. Tulenko, S.R. Phillpot, S.B. Sinnott, J. Nucl. Mater. 384 (2009) 61–69.
[25] A.F. Kohan, G. Ceder, D. Morgan, C.G. Van de Walle, Phys. Rev. B 61 (2000) 15019–15027.
[26] J.W. Christian, The Theory of Transformations in Metals and Alloys, 2nd ed., Pergamon Press, 1975.
[27] G. Kresse, J. Furthmüller, Phys. Rev. B 54 (1996) 11169–11186.
[28] G. Kresse, J. Furthmüller, Comput. Mater. Sci. 6 (1996) 15–50.
[29] G. Kresse, D. Joubert, Phys. Rev. B 59 (1999) 1758–1775.
[30] J.P. Perdew, J.A. Chevary, S.H. Vosko, K.A. Jackson, M.R. Pederson, D.J. Singh, C. Fiolhais, Phys. Rev. B 46 (1992) 6671–6687.
[31] J.P. Perdew, A. Zunger, Phys. Rev. B 23 (1981) 5048–5079.
[32] H.J. Monkhorst, J.D. Pack, Phys. Rev. B 13 (1976) 5188–5192.
[33] A. Solontsov, V. Silin, Phys. Lett. A 334 (2005) 453–459.
[34] A.E. Mattsson, P.A. Schultz, M.P. Desjarlais, T.R. Mattsson, K. Leung, Modell. Simul. Mater. Sci. Eng. 13 (2005) R1–R31.
[35] S. Hayes, J. Thomas, K. Peddicord, J. Nucl. Mater. 171 (1990) 271–288.
[36] X.-J. Chen, V.V. Struzhkin, Z. Wu, M. Somayazulu, J. Qian, S. Kung, A.N. Christensen, Y. Zhao, R.E. Cohen, H.-K. Mao, R.J. Hemley, Proc. Nat. Acad. Sci. USA 102 (2005) 3198–3201.
[37] A.R. Denton, N.W. Ashcroft, Phys. Rev. A 43 (1991) 3161–3164.
[38] R. Benz, M.G. Bowman, J. Am. Chem. Soc. 88 (1966) 264–268.
[39] R. Benz, W. Hutchinson, J. Nucl. Mater. 36 (1970) 135–146.
[40] D.G. Pettifor, Bonding and Structure of Molecules and Solids, Oxford University Press, 1995.
[41] H.W. Hugosson, O. Eriksson, U. Jansson, A.V. Ruban, P. Souvatzis, I.A. Abrikosov, Surface Sci. 557 (2004) 243–254.